How to cite: *Angew. Chem. Int. Ed.* **2022,** *61,* e202210145
International Edition: doi.org/10.1002/anie.202210145
German Edition: doi.org/10.1002/ange.202210145

Palladium Catalysis

Stereoretentive Regio- and Enantioselective Allylation of Isoxazolinones by a Planar Chiral Palladacycle Catalyst

Xin Yu[+], Lingfei Hu[+], Wolfgang Frey, Gang Lu, and René Peters**

Abstract: The catalytic allylic substitution is one of the most important tools in asymmetric synthesis to form C–C bonds in an enantioselective way. While high efficiency was previously accomplished in terms of enantio- and regiocontrol using different catalyst types, a strong general limitation is a very pronounced preference for the formation of allylic substitution products with (*E*)-configured C=C double bonds. Herein, we report that with a planar chiral palladacycle catalyst a diastereospecific reaction outcome is achieved using isoxazolinones and allylic imidates as substrates, thus maintaining the C=C double bond geometry of the allylic substrates in the highly enantioenriched products. DFT calculations show that the reactions proceed via an S_N2 mechanism and not via π-allyl Pd complexes. Crucial for the high control is the stabilization of the allylic fragment in the S_N2 transition state by π-interactions with the phenyl substituents of the pentaphenylferrocenyl catalyst core.

Asymmetric allylic alkylations (AAAs) are widely used in synthetic organic chemistry due to their broad scope regarding suitable classes of nucleophiles and the synthetic versatility of the C=C double bond introduced by the allylic electrophile.[1] High efficiency has been reported for AAAs in terms of regio- and enantiocontrol at the allylic reaction partner.[2] Palladium complexes belong to the most frequently used catalysts.[1] The reactions usually proceed via an oxidative addition of an allylic acetate/carbonate to a Pd^0 catalyst to form an electrophilic cationic π-allyl-Pd complex which is attacked from the outer-sphere by a soft nucleophile.[1]

A limitation in Pd^0 catalyzed AAAs is the fact that the installed allyl moieties always adopt an (*E*)-configuration, whereas (*Z*)-diastereomers are not directly accessible as a

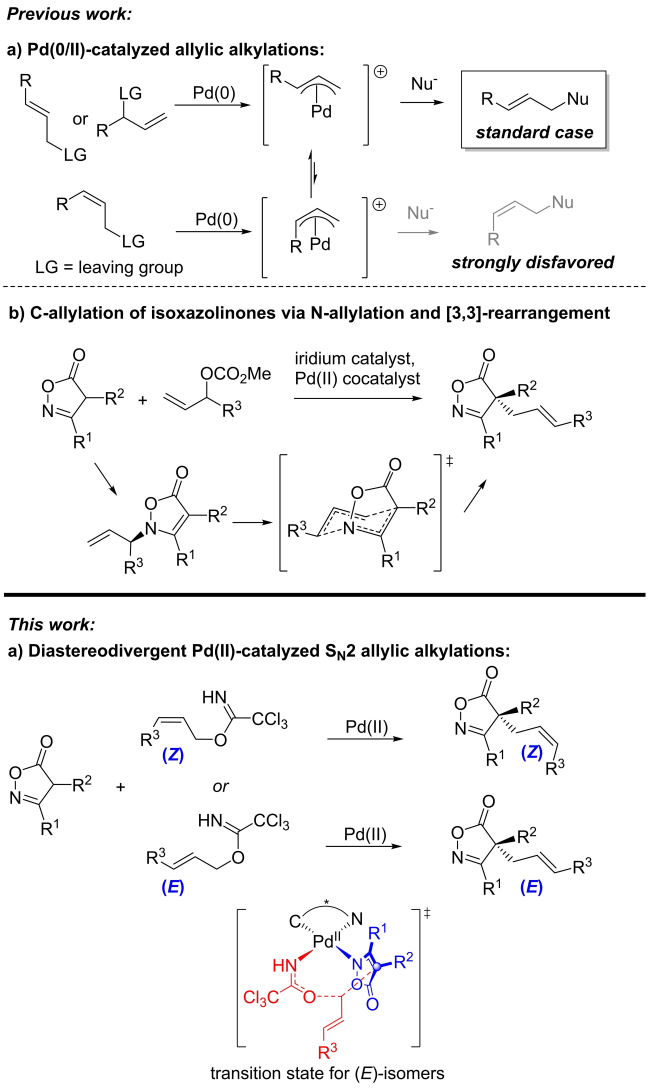

Scheme 1. Comparison of previous work to this work.

[*] Dr. X. Yu,[+] Dr. W. Frey, Prof. Dr. R. Peters
Universität Stuttgart, Institut für Organische Chemie
Pfaffenwaldring 55, 70569 Stuttgart (Germany)
E-mail: rene.peters@oc.uni-stuttgart.de
M.Sc. L. Hu,[+] Prof. Dr. G. Lu
Shandong University, School of Chemistry and Chemical Engineering, Key Laboratory of Colloid and Interface Chemistry, Ministry of Education
Jinan, Shandong 250100 (China)
E-mail: ganglu@sdu.edu.cn
Dr. X. Yu[+]
ZJU-Hangzhou Global Scientific and Technological Innovation Center
Hangzhou, Zhejiang 311200 (China)
[+] These authors contributed equally to this work.

result of a rapid isomerization of the π-allyl-Pd complexes (Scheme 1, top).[3,1,4]

Recently, our group has reported a binary catalyst system consisting of a chiral Ir^{I} complex[5] and an achiral Pd^{II} salt, which allowed for the only reported catalytic asymmetric allylation of isoxazolinones (Scheme 1, middle).[6–8] Isoxazolinones are synthetically versatile heterocycles prepared in one step from β-ketoesters and hydroxylamine,[7b] and can for instance be transformed into biologically interesting β-aminoacid derivatives.[9] It was shown that this allylation proceeded via an Ir catalyzed regioselective N-allylation forming a branched allyl isomer which then undergoes a [3,3]-rearrangement, thereby enforcing an (*E*)-configuration of the C=C double bond.

Herein, we report a diastereospecific catalytic asymmetric C-allylation of isoxazolinones using a planar chiral ferrocene based palladacycle capable of maintaining the double bond geometry of the allylic electrophile within the product (Scheme 1, bottom).

Allylation products possessing a (*Z*)-configured double bond are thus also efficiently available with a high level of diastereo-, enantio- and regiocontrol. DFT (density functional theory) calculations show that the reaction proceeds via a Pd-catalyzed S_N2 reaction rather than the common π-allyl-Pd complexes.

Our palladacycle catalysts were initially developed for asymmetric rearrangements of trifluoroacetimidates to form *N*-acylated allylic amines.[10–12] Still, the corresponding allylic trichloroacetimidates were found to be suitable allylation agents avoiding the rearrangement. Among the metallacycles tested the **p**enta**p**henyl**f**errocene **i**midazoline **p**alladacycle catalyst system (**PPFIP**, entry 4) was the only one that strongly favors the linear over the branched allylation product (Table 1, entries 1–5).

Moreover **PPFIP** was the only catalyst system that induced high enantioselectivity. In initial experiments the precatalysts were activated by AgOAc according to our reported procedure to allow for a chloride/acetate ligand exchange.[10,11] This activation improves the productivity as entry 6 shows. Installation of less basic anionic ligands using different silver salts allowed for similar enantio- and regioselectivities as exemplified by entries 7 & 8, but yields were lower. The use of very weakly coordinating anions such as triflate resulted in poor regio- and enantioselectivity and massive substrate decomposition

Table 1: Development of the title reaction.

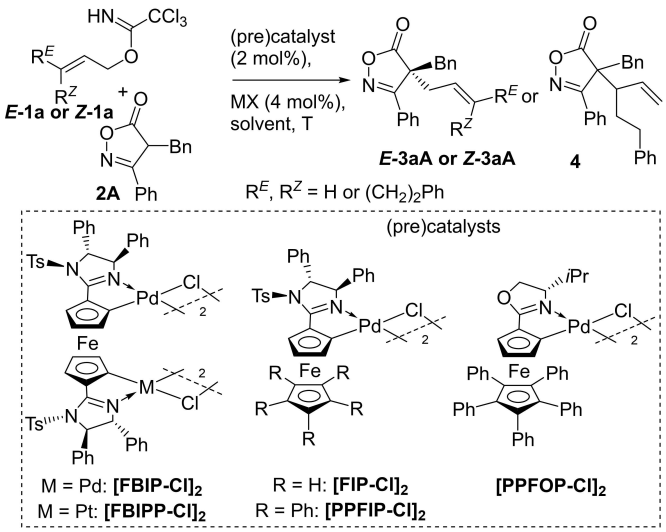

#	Precatalyst/MX	Solvent	***E/Z*-1a**	Yield[a] **3/4** [%]	*E*:*Z*[a] **3**	*ee*[b] **3** [%]
1	**[FIP-Cl]$_2$**/AgOAc	CH_2Cl_2	*E*	7/10	>99:1	13
2	**[FBIP-Cl]$_2$**/AgOAc	CH_2Cl_2	*E*	14/5	>99:1	22
3	**[FBIPP-Cl]$_2$**/AgOAc	CH_2Cl_2	*E*	18/8	>99:1	17
4	**[PPFIP-Cl]$_2$**/AgOAc	CH_2Cl_2	*E*	75/8	>99:1	87
5	**[PPFOP-Cl]$_2$**/AgOAc	CH_2Cl_2	*E*	7/23	>99:1	9
6	**[PPFIP-Cl]$_2$**	CH_2Cl_2	*E*	46/8	>99:1	85
7	**[PPFIP-Cl]$_2$**/AgTFA	CH_2Cl_2	*E*	65/7	>99:1	87
8	**[PPFIP-Cl]$_2$**/AgOMs	CH_2Cl_2	*E*	64/6	>99:1	88
9	**[PPFIP-Cl]$_2$**/AgOTf	CH_2Cl_2	*E*	28/14	>99:1	34
10	**[PPFIP-Cl]$_2$**/Na(acac)	CH_2Cl_2	*E*	89/7	>99:1	90
11	**[PPFIP-Cl]$_2$**/Na(acac)	$CHCl_3$	*E*	91/5	>99:1	91
12	**[PPFIP-Cl]$_2$**/Na(acac)	$CHCl_3$	*Z*	89/6	1:22	99

[a] Determined by ^{1}H NMR using mesitylene as an internal standard. [b] Enantiomeric excess of the major geometrical isomer determined by HPLC. OAc: acetate; TFA: trifluoroacetate, OMs: methanesulfonate; OTf: trifluoromethanesulfonate; acac: acetylacetonate.

(entry 9). As a practical alternative, silver free activation by Na(acac) led to high product yield with good linear/branched selectivity and high enantioselectivity (entry 10). Small improvements were found using $CHCl_3$ as solvent (entry 11). The same conditions could also be applied to the *Z*-configured allylic imidate ***Z*-1a** ($R^Z=(CH_2)_2Ph$, $R^E=H$), with the *Z*-configuration being maintained in the nearly enantiopure product (entry 12).

The optimized conditions were applied to various substrates with different residues R^1-R^3, R^E and R^Z (Table 2). In most cases, the double bond geometry was conserved to a large degree. In general, enantioselectivity was particularly high for *Z*-configured substrates (entries marked with blue color) usually attaining 99% ee (15 examples). *Z*/*E* ratios between 8:1 and 73:1 were commonly found in the products. A lower ratio was found for substrate ***Z*-1h** carrying a Ph ring as R^Z.[13]

With *E*-configured allylic substrates, enantioselectivity was a bit lower with up to 94% *ee*. A particularly difficult reaction was the synthesis of ***E*-3aI**, employing an isoxazolinone substrate carrying a C–H acidic Me residue R^2 (72% *ee*). For comparison, ***Z*-3aI** was formed in almost enantiopure form, but *E*/*Z*-isomerization was more significant than otherwise (*Z*/*E*=3:1). Difficult is the enantiocontrol with strong π-acceptors in R^2, maybe because enolization depends less on the catalyst in this case (see ***E*-3aM**).

Functionalized allylic substrates carrying, e.g., ester, ether, nitrile, carbamate, ketone or additional olefin moieties within aliphatic chains were tolerated. Noteworthy is also the reactivity with an allylic substrate featuring a Me group R^1 (***E*-1o** and ***Z*-1p**), because substrates of this type showed no reactivity in allylic imidate rearrangements using this catalyst type.[10]

To gain insight into the reaction mechanism, several control experiments were conducted. Previously, some catalytic asymmetric reactions using trichloroacetimidates and palladacycle catalysts were reported, in which competing imidate rearrangements could be kinetically outperformed.[14] These studies revealed that the corresponding C–O bond forming reactions follow a Pd^{II} catalyzed S_N2' mechanism favoring branched products.[15,16]

In contrast, in our case the C–C bond formation occurs at the allylic C atom carrying the imidate leaving group thus forming a linear product. To rule out an S_N2' mechanism we investigated allylic imidate rearrangement product **5** as possible intermediate, but **3aA** was not formed under the reaction conditions (Scheme 2, top). In addition, the branched allylimidate **6** led mainly to the *N*-allylation product next to small amounts of ***E*-3aA** (Scheme 2, middle), which was formed with low enantioselectivity. No allylation products were formed with allylic carbonates or acetates (not shown).

Moreover, we considered the option of an *N*-allylation with a subsequent [3,3]-rearrangement.[14b] However, substrate **8**[6] did not form **3aA** under the reaction conditions (Scheme 2, bottom), no matter if trichloroacetamide was present or not.

Table 2: Investigation of the substrate scope.[a]

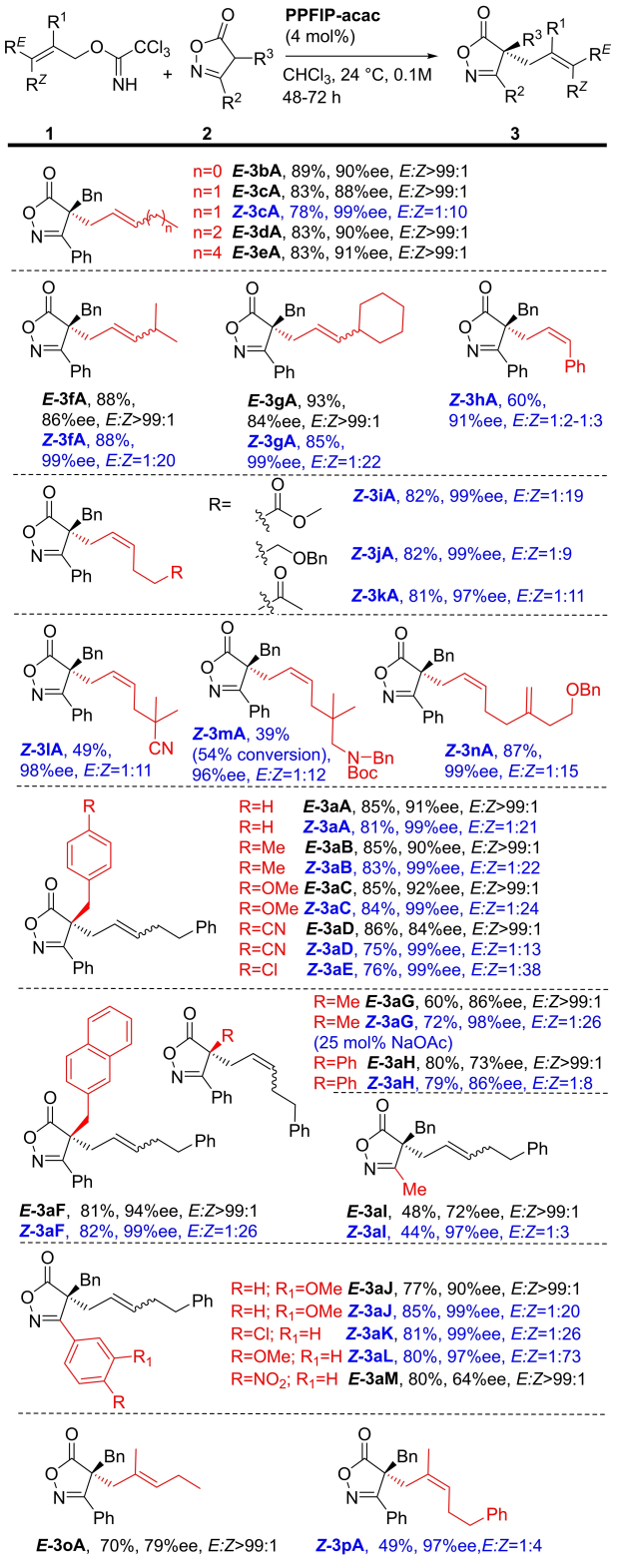

[a] Yields of isolated products after column chromatography, ee determined by HPLC, *E*:*Z* ratios determined by ^1H NMR from the crude product.

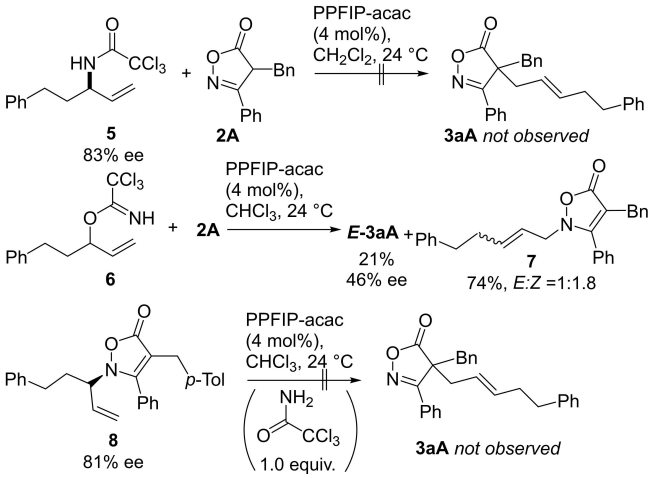

Scheme 2. Control experiments.

DFT calculations were performed to understand this reaction type (for computational details see the Supporting Information). The computed free energy profile is shown in Figure 1. The reaction commences with the C–H activation with Pd^{II} via a CMD (concerted metalation deprotonation) mechanism with a barrier of 20.4 kcal mol^{-1} (**TS1**), generating the N-bound Pd^{II} intermediate (**int3**) rather than the C-bound Pd^{II} species (see details in Supporting Information). The subsequent ligand exchange with *E*-allylic imidate ***E*-1b** gives the more stable **int4**. In principle, **int4** could undergo a C–O oxidative addition and a subsequent C–C reductive elimination to deliver the C-allylation product. However, the computed transition state of C–O oxidative addition is highly disfavored (**TS2c**, $\Delta G^{\ddagger} = 31.4$ kcal mol^{-1} with respect to **int4**), indicating the formation of a Pd^{IV} intermediate is less preferred. Instead, we found a concerted pathway. The relatively low barrier of **TS2a** ($\Delta G^{\ddagger} = 17.7$ kcal mol^{-1} with respect to **int4**) suggests the C–C bond formation proceeds via an S_N2 mechanism. Based on this mechanism, the configuration of allylic imidates can be transferred to the allyl products, which is in line with the experimental observations (Table 1).

The irreversible S_N2 allylation step determines the enantioselectivity of this reaction. The barrier difference between **TS2a** and **TS2b** with **PPFIP** ($\Delta\Delta G^{\ddagger} =$ 3.2 kcal mol^{-1}) is consistent with the experimentally observed high-level enantioselectivity (entry 11, Table 1). As shown in Figure 2, the barrier difference is mostly due to the difference in non-covalent interactions between the two transition states (see details in Supporting Information). In the favored **TS2a**, the stabilizing π···π interactions include allyl-phenyl and phenyl-phenyl interactions (highlighted in green and yellow). In contrast, the disfavored **TS2b** only has one phenyl-phenyl interaction. The lack of these stabilizing π···π interactions in other palladacycle catalysts, such as **FIP** and **PPFOP**, leads to low ee values (entries 1 and 5, Table 1).

In conclusion, we have reported a diastereospecific catalytic enantioselective allylic substitution, enabled by a planar chiral pentaphenylferrocenyl imidazoline palladacycle catalyst. Cyclic oxime esters reacted with allylic trichloroacetimidates in a way that the double bond geometry of the allylic substrate is maintained in the allylic substitution products. The latter were formed with high enantio- and regiocontrol. DFT calculations strongly favor a concerted S_N2 pathway and rule out pathways via

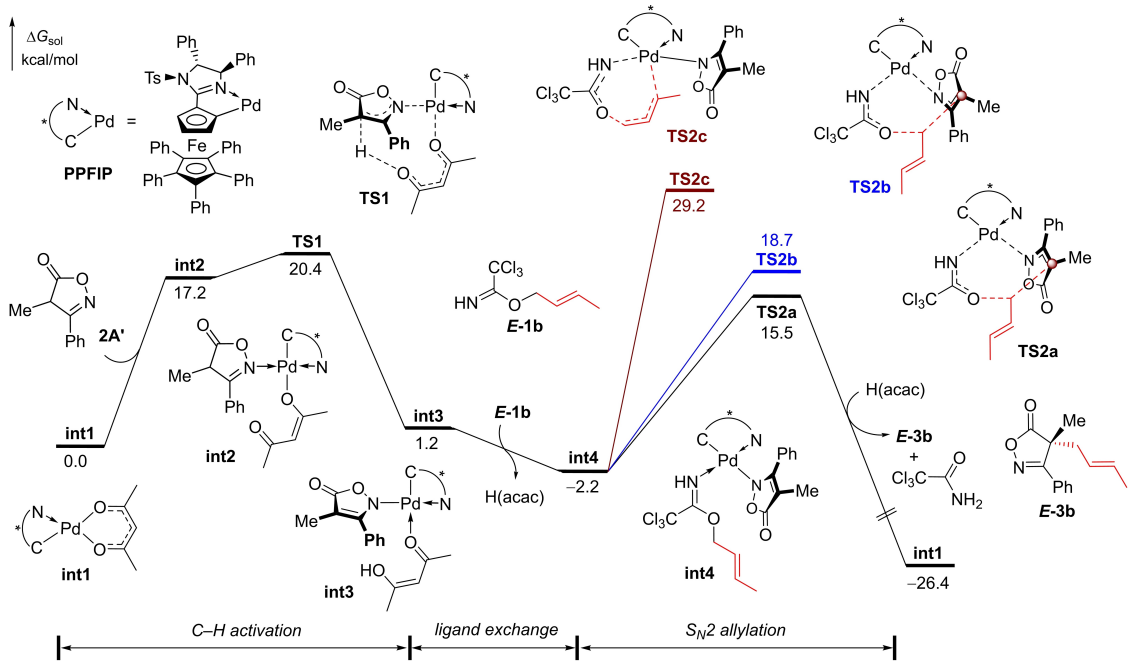

Figure 1. DFT-computed energy profile for Pd-catalyzed allylation of isoxazolinones. Energies are computed at the M06/SDD-6-311+G(d,p)/SMD($CHCl_3$) level of theory with geometries optimized at the B3LYP/LANL2DZ-6-31G(d) level.

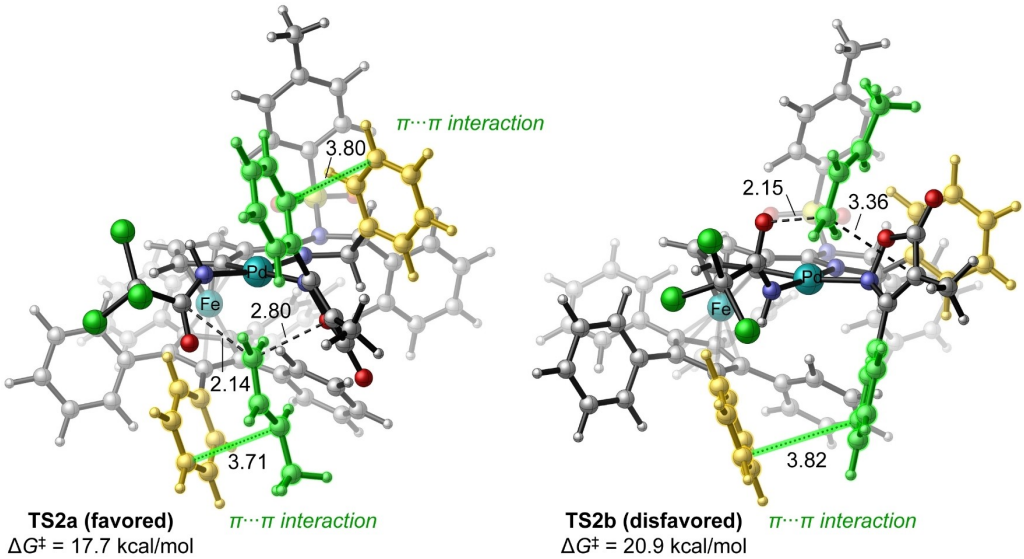

Figure 2. Optimized geometries of S_N2 allylation transition states. Key bond lengths are shown in Å.

π-allyl-Pd complexes. Essential for the high efficiency in terms of regio- and enantiocontrol is the stabilization of the allylic fragment in the S_N2 transition state by π-interactions with the phenyl substituents of the pentaphenylferrocenyl catalyst core.

Acknowledgements

This work was financially supported by the Deutsche Forschungsgemeinschaft (DFG, PE 818/4-2). Xin Yu thanks the China Scholarship Council (CSC) for a Ph.D. scholarship. G.L. thanks for the financial support from National Natural Science Foundation of China (No. 21973055), Natural Science Foundation of Shandong Province (ZR2019MB049), Taishan Scholar of Shandong Province (No. tsqn201812013) and Qilu Young Scholar of Shandong University. DFT calculations were performed at the HPC Cloud Platform of Shandong University. Open Access funding enabled and organized by Projekt DEAL.

Conflict of Interest

The authors declare no conflict of interest.

Data Availability Statement

The data that support the findings of this study are available in the Supporting Information of this article.

Keywords: Regioselective · Allylic Substitution · Asymmetric Catalysis · Diastereospecific · Palladium

[1] Selected reviews: a) G. Helmchen, *Asymmetric Allylic Substitutions in Asymmetric Synthesis* (Eds.: M. Christmann, S. Bräse), Wiley-VCH, Weinheim, **2008**, pp. 102–106; b) Z. Lu, S. Ma, *Angew. Chem. Int. Ed.* **2008**, *47*, 258–297; *Angew. Chem.* **2008**, *120*, 264–303; c) L. Milhau, P. J. Guiry, *Top. Organomet. Chem.* **2011**, *38*, 95–154; d) G. Poli, G. Prestat, F. Liron, C. Kammerer-Pentier, *Top. Organomet. Chem.* **2011**, *38*, 1–63; e) B. M. Trost, D. L. Van Vranken, *Chem. Rev.* **1996**, *96*, 395–422.

[2] Selected reviews: a) G. Helmchen, *Iridium Complexes in Organic Synthesis*, Wiley-VCH, Weinheim, **2009**, pp. 211–250; b) G. Helmchen, A. Dahnz, P. Duebon, M. Schelwies, R. Weihofen, *Chem. Commun.* **2007**, *7*, 675–691; c) M. Diéguez, O. Pàmies, *Acc. Chem. Res.* **2010**, *43*, 312–322; d) K. Geurts, S. P. Fletcher, A. W. van Zijl, A. J. Minnaard, B. L. Feringa, *Pure Appl. Chem.* **2008**, *80*, 1025–1037; e) J.-L. Renaud, B. Demerseman, M. D. Mbaye, C. Bruneau, *Curr. Org. Chem.* **2006**, *10*, 115–133; f) G. Helmchen, A. Pfaltz, *Acc. Chem. Res.* **2000**, *33*, 336–345; g) B. Sundararaju, M. Achard, C. Bruneau, *Chem. Soc. Rev.* **2012**, *41*, 4467–4483; h) B. M. Trost, M. L. Crawley, *Chem. Rev.* **2003**, *103*, 2921–2944.

[3] For an interesting approach, which used enantioenriched substrates for asymmetric induction, in which the (*Z*)-geometry could be retained, see: K. Krämer, U. Kazmaier, *J. Org. Chem.* **2006**, *71*, 8950–8953.

[4] For Ir catalysis, a Z-selective version was recently developed: R. Jiang, L. Ding, C. Zheng, S.-L. You, *Science* **2021**, *371*, 380–386.

[5] a) S. Spiess, C. Welter, G. Franck, J.-P. Taquet, G. Helmchen, *Angew. Chem. Int. Ed.* **2008**, *47*, 7652–7655; *Angew. Chem.* **2008**, *120*, 7764–7767; b) J. Qu, G. Helmchen, *Acc. Chem. Res.* **2017**, *50*, 2539–2555; c) J. A. Raskatov, M. Jäkel, B. F. Straub, F. Rominger, G. Helmchen, *Chem. Eur. J.* **2012**, *18*, 14314–14328; d) K.-Y. Ye, L.-X. Dai, S.-L. You, *Org. Biomol. Chem.* **2012**, *10*, 5932–5939; e) X. Jiang, J. J. Beiger, J. F. Hartwig, *J. Am. Chem. Soc.* **2017**, *139*, 87–90; f) W. Chen, J. F. Hartwig, *J. Am. Chem. Soc.* **2013**, *135*, 2068–2071; g) W.-B. Liu, C. Zheng, C.-X. Zhuo, L.-X. Dai, S.-L. You, *J. Am. Chem. Soc.* **2012**, *134*, 4812–4821; h) W.-B- Liu, J.-B. Xia, S.-L. You, *Top. Organomet. Chem.* **2012**, *38*, 155–207; i) J. F. Hartwig, L. M. Stanley, *Acc. Chem. Res.* **2010**, *43*, 1461–1475.

[6] S. Rieckhoff, J. Meisner, J. Kästner, W. Frey, R. Peters, *Angew. Chem. Int. Ed.* **2018**, *57*, 1404–1408; *Angew. Chem.* **2018**, *130*, 1418–1422.

[7] For other applications of isoxazolinones in asymmetric catalysis, see: a) W.-T. Meng, Y. Zheng, J. Nie, N.-Y. Xiong, J.-A. Ma, *J. Org. Chem.* **2013**, *78*, 559–567; b) T. Hellmuth, W. Frey, R. Peters, *Angew. Chem. Int. Ed.* **2015**, *54*, 2788–2791; *Angew. Chem.* **2015**, *127*, 2829–2833; c) H. Zhang, B. Wang, L. Cui, X. Bao, J. Qu, Y. Song, *Eur. J. Org. Chem.* **2015**, 2143–2147.

[8] Recent reviews for synthetic applications of isoxazolinones: a) A. Macchia, A. Eitzinger, J.-F. Brière, M. Waser, A. Massa, *Synthesis* **2021**, *53*, 107–122; b) A. F. da Silva, A. A. G. Fernandes, S. Thurow, M. L. Stivanin, I. D. Jurberg, *Synthesis* **2018**, *50*, 2473–2489; Early studies: c) K. Okamoto, T. Oda, S. Kohigashi, K. Ohe, *Angew. Chem. Int. Ed.* **2011**, *50*, 11470–11473; *Angew. Chem.* **2011**, *123*, 11672–11675; d) K. Okamoto, T. Shimbayashi, E. Tamura, K. Ohe, *Chem. Eur. J.* **2014**, *20*, 1490–1494; e) S. Rieckhoff, T. Hellmuth, R. Peters, *J. Org. Chem.* **2015**, *80*, 6822–6830; f) K. Okamoto, T. Shimbayashi, M. Yoshida, A. Nanya, K. Ohe, *Angew. Chem. Int. Ed.* **2016**, *55*, 7199–7202; *Angew. Chem.* **2016**, *128*, 7315–7318; g) S. Rieckhoff, M. Titze, W. Frey, R. Peters, *Org. Lett.* **2017**, *19*, 4436–4439; h) T. Shimbayashi, G. Matsushita, A. Nanya, A. Eguchi, K. Okamoto, K. Ohe, *ACS Catal.* **2018**, *8*, 7773–7780; i) S. Rieckhoff, W. Frey, R. Peters, *Eur. J. Org. Chem.* **2018**, 1797–1805.

[9] a) N. Wannenmacher, C. Pfeffer, W. Frey, R. Peters, *J. Org. Chem.* **2022**, *87*, 670–682; b) N. Wannenmacher, N. Keim, W. Frey, R. Peters, *Eur. J. Org. Chem.* **2022**, e202200030; for related approaches, see also; c) J.-S. Yu, H. Noda, M. Shibasaki, *Angew. Chem. Int. Ed.* **2018**, *57*, 818–822; *Angew. Chem.* **2018**, *130*, 826–830; d) M. Nascimento de Oliveira, S. Arseniyadis, J. Cossy, *Chem. Eur. J.* **2018**, *24*, 4810–4814; e) V. Capaccio, K. Zielke, A. Eitzinger, A. Massa, L. Palombi, K. Faust, M. Waser, *Org. Chem. Front.* **2018**, *5*, 3336–3340.

[10] a) M. E. Weiss, D. F. Fischer, Z.-Q. Xin, S. Jautze, W. B. Schweizer, R. Peters, *Angew. Chem. Int. Ed.* **2006**, *45*, 5694–5698; *Angew. Chem.* **2006**, *118*, 5823–5827; b) Z.-Q. Xin, D. F. Fischer, R. Peters, *Synlett* **2008**, 1495–1499; c) D. F. Fischer, A. Barakat, Z.-Q. Xin, M. E. Weiss, R. Peters, *Chem. Eur. J.* **2009**, *15*, 8722–8741; d) R. Peters, Z.-Q. Xin, F. Maier, *Chem. Asian J.* **2010**, *5*, 1770–1774; e) J. M. Bauer, R. Peters, *Catal. Sci. Technol.* **2015**, *5*, 2340–2346.

[11] Selected further applications of these catalysts: a) J. M. Bauer, W. Frey, R. Peters, *Angew. Chem. Int. Ed.* **2014**, *53*, 7634–7638; *Angew. Chem.* **2014**, *126*, 7764–7768; b) C. Schrapel, R. Peters, *Angew. Chem. Int. Ed.* **2015**, *54*, 10289–10293; *Angew. Chem.* **2015**, *127*, 10428–10432; c) X. Yu, N. Wannenmacher, R. Peters, *Angew. Chem. Int. Ed.* **2020**, *59*, 10944–10948; *Angew. Chem.* **2020**, *132*, 11037–11041.

[12] For reviews on ferrocenyl palladacycles in asymmetric catalysis, see: a) C. J. Richards in *Chiral Ferrocenes in Asymmetric Catalysis* (Eds.: L.-X. Dai, X.-L. Hou), Wiley-VCH, Weinheim, **2010**, pp. 337–368; b) H. Nomura, C. J. Richards, *Chem. Asian J.* **2010**, *5*, 1726–1740; c) R. Peters, D. F. Fischer, S. Jautze, *Top. Organomet. Chem.* **2011**, *33*, 139–175.

[13] The absolute configuration of ***E*-3aB** and ***Z*-3aA** was determined by X-ray single crystal structure analysis. Deposition Numbers 1898424 (for ***E*-3aB**) and 1898423 (for ***Z*-3aA**) contain the supplementary crystallographic data for this paper. These data are provided free of charge by the joint Cambridge Crystallographic Data Centre and Fachinformationszentrum Karlsruhe Access Structures service.

[14] a) J. S. Cannon, L. E. Overman, *Acc. Chem. Res.* **2016**, *49*, 2220–2231; b) N. Wannenmacher, M. Heberle, X. Yu, A. Demircan, D. M. Wanner, C. Pfeffer, R. Peters, *Adv. Synth. Catal.* **2022**, https://doi.org/10.1002/adsc.202200185.

[15] a) J. S. Cannon, S. F. Kirsch, L. E. Overman, H. F. Sneddon, *J. Am. Chem. Soc.* **2010**, *132*, 15192–15203.

[16] Moreover, the substrate class has been described for Rh or Ir catalyzed allylic substitutions to form C–X bonds in branched allylic regioisomers: J. S. Arnold, Q. Zhang, H. M. Nguyen, *Eur. J. Org. Chem.* **2014**, 4925–4948.

Manuscript received: July 11, 2022
Accepted manuscript online: July 28, 2022
Version of record online: August 19, 2022